A R C H I V E S O F M E T A L L U R G Y A N D M A T E R I A L S
Volume 57 2012 Issue 2
DOI: 10.2478/v10172-012-0063-y

J. KRAWCZYK*, A. ŁUKASZEK-SOŁEK*, T. ŚLEBODA*, P. BAŁA*, S. BEDNAREK*, M. WOJTASZEK*

STRAIN INDUCED RECRYSTALLIZATION IN HOT FORGED INCONEL 718 ALLOY

REKRYSTALIZACJA STOPU INCONEL 718 INDUKOWANA ODKSZTAŁCENIEM PODCZAS KUCIA MATRYCOWEGO

Changes in the microstructure of Inconel 718 resulting from hot forging were investigated in this work. Axisymmetrical forging characterized by the areas of different forging reduction ratios was subjected to the analysis. The investigated alloy was forged under various thermomechanical conditions. Two forging modes, differing by the geometry and the temperature of the billet were performed in industrial conditions. It was revealed, that the microstructure of the alloy after forging was in the solutionized condition with different levels of recrystallization determining the differences in the grain size.

Moreover, numerous simulations of the analyzed forging process taking into account variable thermomechanical conditions were performed using QForm 3D v. 5.1 software. The results of the simulations were compared with the results of forging the investigated alloy in industrial conditions. These results showed to be in very good agreement with the experimental observations. The changes in the microstructure of the investigated alloy forging were also compared with the results of the performed simulations. This study allowed determining both the influence of chosen thermomechanical parameters on recrystallization process in hot forged Inconel 718 alloy as well as the possibility of obtaining good quality forgings with uniform microstructure out of this alloy.

Keywords: Inconel 718, hot forging, recrystallization, microstructure, simulations

W pracy przedstawiono wyniki badań zmian w mikrostrukturze stopu Inconel 718 powstałych w wyniku kucia. Kształtowano odkuwkę o kształcie zbliżonym do osiowosymetrycznego będącej jednocześnie przykładem odkuwki posiadającej obszary charakteryzujące się różnym stopniem przerobu materiału. Pozwoliło to uzyskać złożone warunki termomechaniczne podczas kucia i po jego zakończeniu. Zastosowano dwa różne wymiary wsadu oraz dwie różne temperatury nagrzania do kucia. Stwierdzono, że po kuciu mikrostruktura stopu jest w stanie przesyconym z różnym stopniem zaawansowania procesu rekrystalizacji oraz wielkości ziarna po rekrystalizacji.

Przeprowadzono również szereg symulacji procesu kucia omawianego materiału w zmiennych warunkach cieplno-mechanicznych z zastosowaniem programu QForm 3D v. 5.1. Odniesienie wyników modelowania numerycznego analizowanego procesu przeróbki plastycznej do uzyskanej mikrostruktury odkuwki pozwoliło na przedstawienie koncepcji roli warunków termomechanicznych na proces rekrystalizacji w stopie Inconel 718 oraz określenie możliwości kształtowania odkuwki z tego stopu w celu uzyskania jednorodnej mikrostruktury.

1. Introduction

Thermomechanical processing enables obtaining final products by shaping the preforms in various processing routes. The mechanical properties of the obtained products strongly depend on their microstructure. That is why the precise control of all processing steps is necessary.

Inconel 718 alloy is a precipitation strengthened nickel alloy. It is widely used for many industrial applications due to its unique properties. This alloy is well suited for applications requiring high strength in temperature ranges from cryogenic up to 1200°C and that is why it finds application in gas turbine components, nuclear reactors and pumps. It has good forgeability and it is corrosion resistant in the temperatures up to 650°C. Relatively high content of iron combined with low content of cobalt makes the price of this alloy attractive as compared to other nickel alloys [1]. This alloy is commonly delivered in solutionized, ready to ageing condition [2].

Common heat treatment of this alloy consists of:

- Solution treatment usually performed by annealing at the temperature of 924÷1010°C during minimum 0.5 h and air cooling.

* AGH UNIVERSITY OF SCIENCE AND TECHNOLOGY, FACULTY OF METALS ENGINEERING AND INDUSTRIAL COMPUTER SCIENCE, 30-059 KRAKÓW, 30 MICKIEWICZA AV., POLAND

♣ Ageing at 718±14°C during 8 h, cooling in the furnace to 621±14°C and holding at this temperature for 18 h and air cooling [2].

Because recommended annealing temperature range is quite wide and its maximum time is not fixed, the grain size in this alloy can be controlled by proper control of annealing temperature and time [3]. After heat treatment, the microstructure of Inconel 718 alloy constists of many phases. It contains grains of the alloy matrix (γ phase) and γ' and γ" phase precipitations. Precise heat treatment, leading to dissolution of all carbides and precipitation of δ phase instead of γ" phase, is very important [1].

Inconel 718 alloy is usually processed by cold rolling, hot rolling or forging. Forging is more preferred when parts that are more complex need to be produced. The forging temperature for this alloy is about 1065°C. Forging should result in Inconel 718 alloy product with uniform, recrystallized microstructure [1].

The matrix of the alloy, mainly composed of γ grains, determines the strength of the alloy, which also depends on the grain size. It also ensures good plasticity of this alloy [1,4]. γ' and γ" phases are the main phases strengthening this alloy. They also influence the overall strength of this alloy at elevated temperatures [3,5]. Carbides strengthen nickel-based alloys and are responsible for the control of the grain size [1,5-8]. δ phase is also very important while its precipitations on the grain boundaries restrict grain growth during hot processing. This phase can precipitate instead of γ" phase during heat treatment, what is undesirable phenomenon in these alloys [1,5]. Final products made of Inconel alloys are often covered with protective layers to enhance its corrosion resistance at elevated or high temperatures [9,10].

2. Material for testing

Inconel 718 alloy rod with diameter of 50 mm was used as a starting material for the investigations. The chemical composition of the alloy is shown in Table 1. The microstructure of the investigated alloy showed, that it was partly annealed (Fig. 1), what was confirmed by X-ray analysis (Fig. 2). The following phases were identified in the investigated alloy:

- Alloy matrix – γ phase,
- $NbNi_3$ – δ phase,
- Ni_3Nb – γ" phase,
- Ni_3Mo – most probably ε phase,
- NbC and TiC carbides.

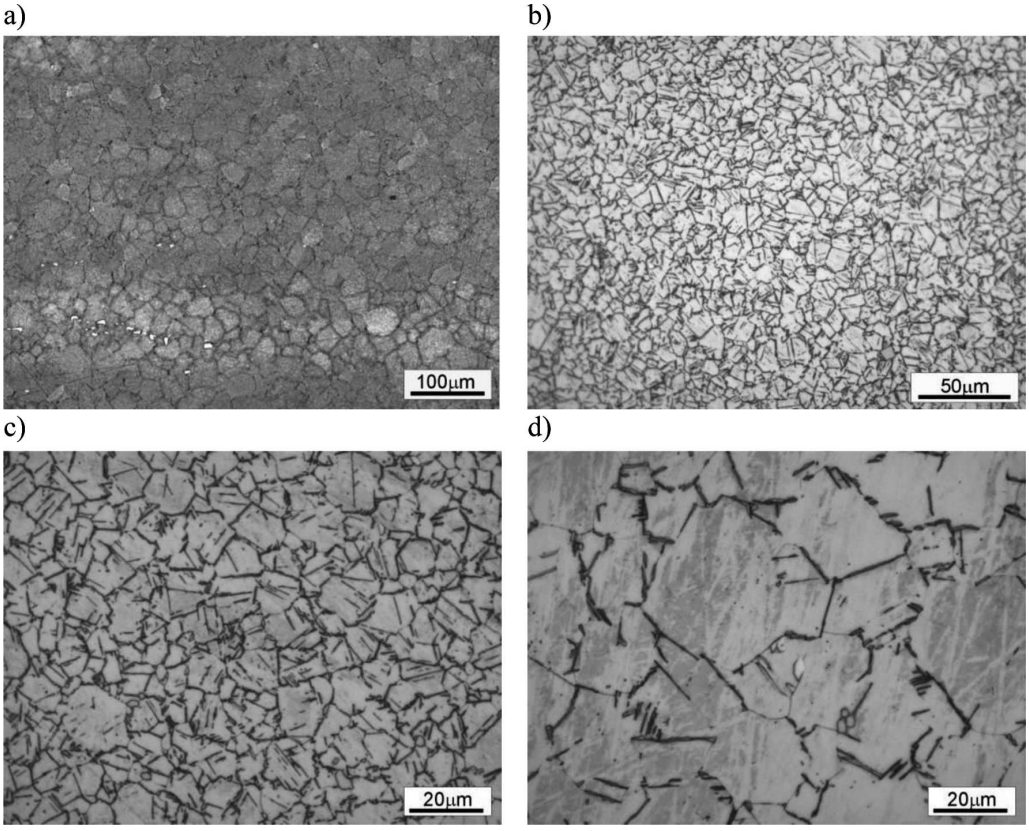

Fig. 1. Microstructure of investigated alloy (as delivered conditions): a) longitudinal cross-section, b,c) transverse cross-section – near the lateral surface of the rod, d) transverse cross-section – near the symmetry axis of the rod

TABLE 1

Chemical composition (weight %) of the investigated Inconel 718 alloy

C	Fe	Co	Nb+Ta	Ti	Cr	Mo	Al	Ni
0.024	18.12	0.20	5.22	1.00	17.95	2.90	0.49	Bal.

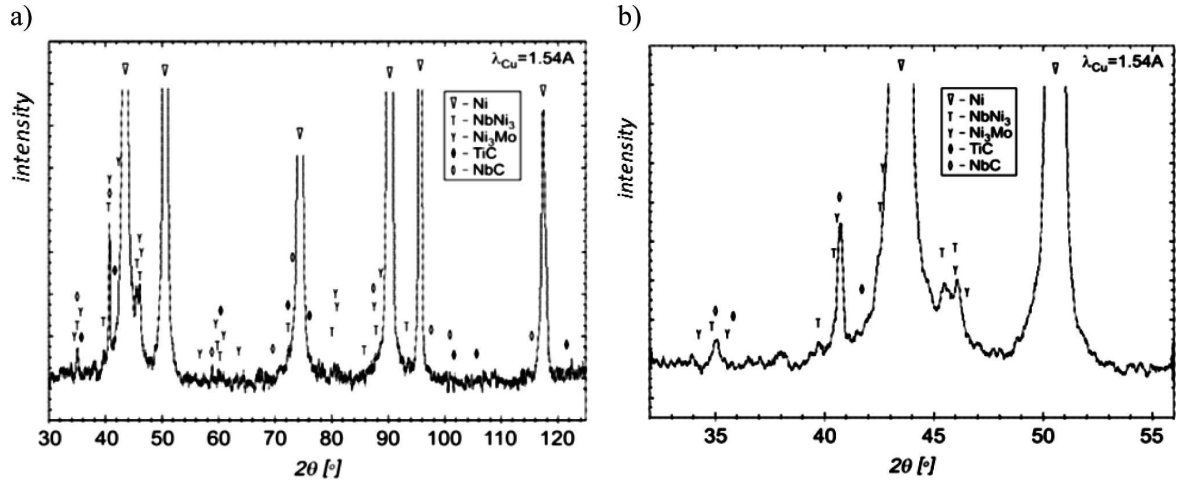

Fig. 2. Diffraction pattern of Inconel 718 alloy – as delivered condition (in 30-125° angle range and in 30-55° angle range, and with variable intensities showing diffraction patterns coming from trace phases)

3. Experimental procedure

Four forgings of Inconel 718 alloy were obtained during forging the billets of different geometries and at various temperatures. The alloy was forged at 1000°C and at 1100°C. The billet was heated up to 1120°C in electric furnace. In the case of forging at 1100°C, the billet was transferred from the furnace into the die cavity and then forged. In the case of forging at 1000°C, the billet after removal from the furnace was cooled down to deformation temperature. The temperature of the billet was constantly monitored by thermocouples attached to it. WG 1262 graphite lubricant was used to lubricate the dies. Inconel 718 alloy billet was covered with silica based Thermex GL lubricant prior to deformation. Inconel 718 alloy forging temperature and billet dimensions are shown in Table 2. Axisymmetric collar was chosen as final forging geometry (Fig. 3). Such geometry of the final product ensured different forging reduction ratios and various local thermomechanical conditions during processing. The samples for metallographic investigations were taken from each selected areas of four produced forgings according to Fig. 4. Cross-sections A and B with marked areas of microstructure observations and hardness measurements are shown in Fig. 5. Samples were etched with etchant: 4g $CuSO_4$+ 20 ml HCl + 20 ml C_2H_5OH.

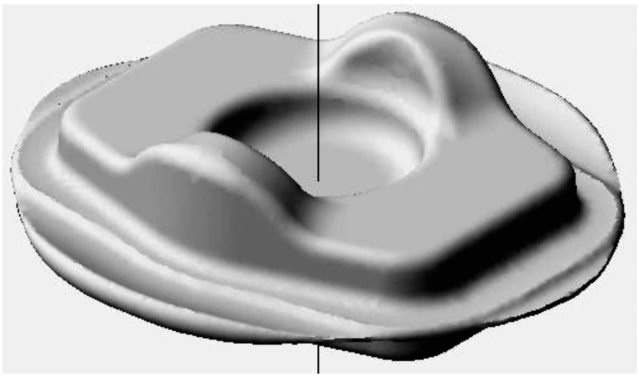

Fig. 3. Numerical model of Inconel 718 alloy forging

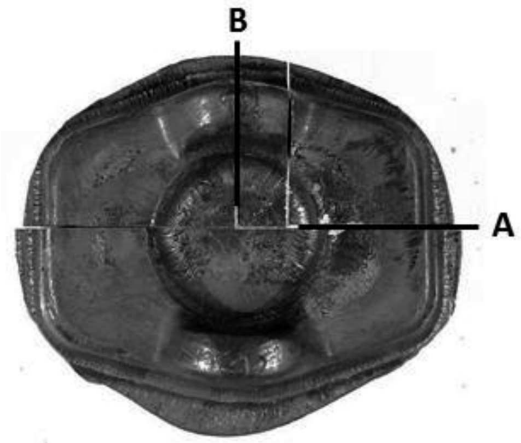

Fig. 4. Inconel 718 alloy forging with marked cross-sections (A and B) for metallographic investigations

TABLE 2

Inconel 718 alloy forging temperature and billet dimensions

No. of sample	Forging temperature, °C	Diameter of the billet, mm	Height of the billet, mm
1.	1100	35	49
2.	1000	35	49
3.	1100	50	30
4.	1000	50	30

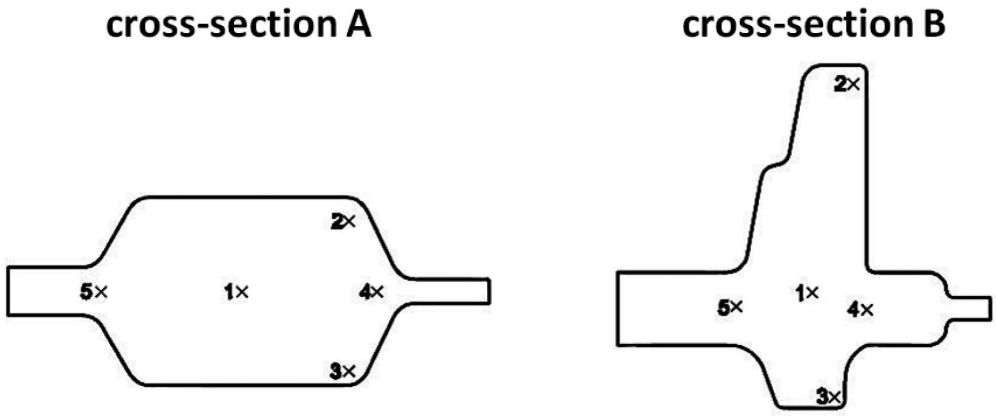

Fig. 5. Cross-sections A and B with marked (x) and numbered areas of microstructure and hardness analysis

4. Numerical modeling

Experimental investigations were preceded by detailed analysis of numerical model of the analyzed forging process using QForm3D software. The analyzed material flow characteristics, necessary for the forging process simulations, was determined by compression tests under various temperature-stress-strain conditions using Gleeble 3800 thermomechanical simulator. Effective strain, mean stress and temperature distributions were obtained from the performed simulations. An elastic-viscoplastic model of the material and Levanov's friction model were assumed in the numerical simulations.

The results of numerical modeling of forging Inconel 718 billet are presented in Figures 6 and 7. The temperature distribution (Fig. 6) and effective strain

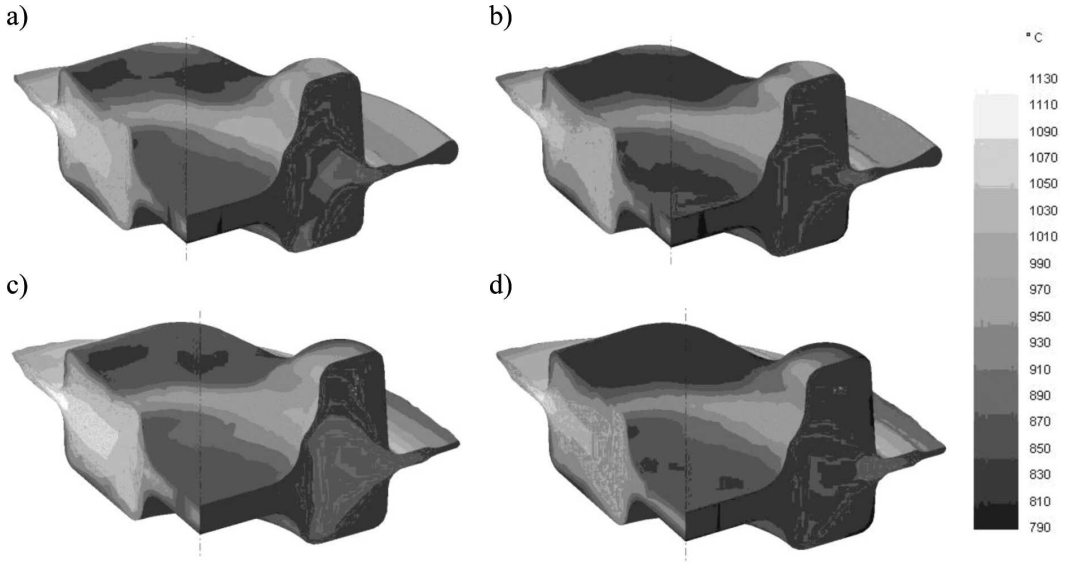

Fig. 6. Temperature distribution in Inconel 718 alloy forged: a) sample No. 1, b) sample No. 2, c) sample No. 3, d) sample No. 4

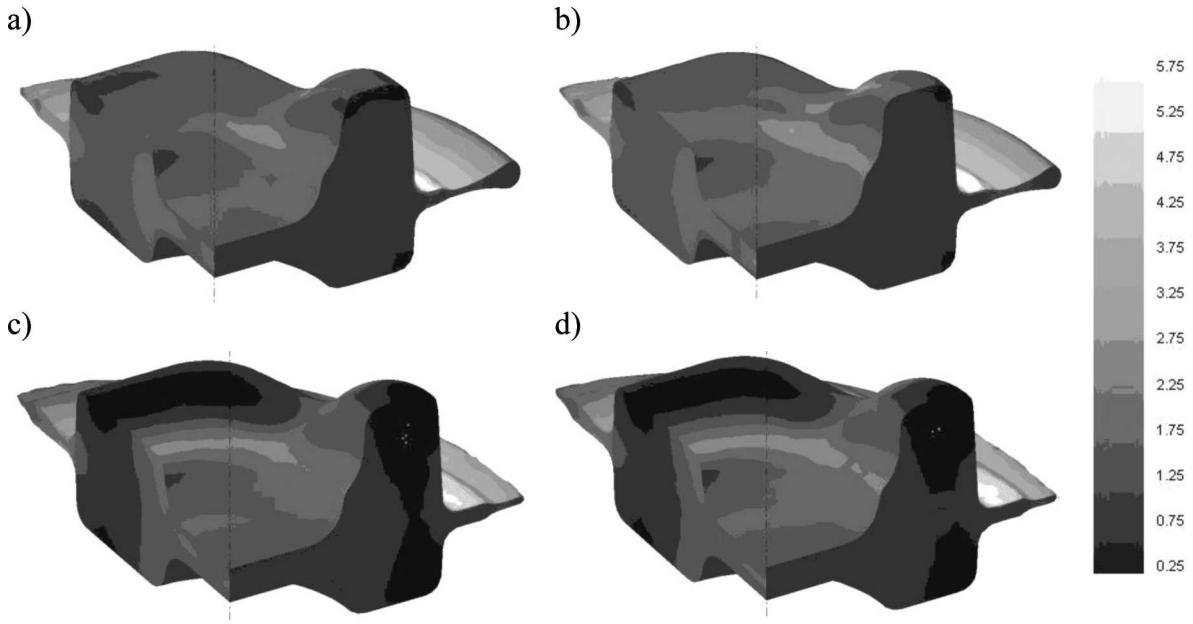

Fig. 7. Effective strain distribution in Inconel 718 alloy forging: a) sample No. 1, b) sample No. 2, c) sample No. 3, d) sample No. 4

(Fig. 7) were analyzed in the forging cross-sections. The results of the numerical modelling show many differences in the temperature and strain distributions in the analyzed forgings. The application of the billet of smaller diameter causes, despite of greater forging ratio, lower overall increases in the temperature of the billet during forging, what is most probably connected with more intense heat transfer from the billet to forging dies.

5. Results and discussion

The microstructure of the forgings mostly consists of the solutionized alloy matrix (Fig. 8) and precipitations of carbides (Fig. 9). Depending on the forging temperature and forging ratio (higher in the case of smaller diameter of the billet) as well as on the area of the analyzed forgings (for cross-sections A and B the areas 5, 4, 1, 3, 2 (Fig. 10 and Fig. 11) respectively), forging ration increases leading to different extend of recrystallization. Recrystallization starts on grain boundaries as shown in Fig. 12. An increase of forging temperature causes more intense recrystallizing of the alloy (Fig. 13). The same effect could be noticed in the case of the increasing strain (Fig. 14). In some areas of the processed alloy lower strain or local increase of the temperature resulted in grain growth (Fig. 15 and Fig. 16). The observations of the microstructure of the obtained forgings did not reveal any nucleates of new grains on twin boundaries, which can be (potentially in second order [11]) the areas of nucleation (Fig. 17). Unrecrystallized areas were also observed, but only in the forgings processed at 1000°C and only in the areas of lowest strain intensity (Fig. 18).

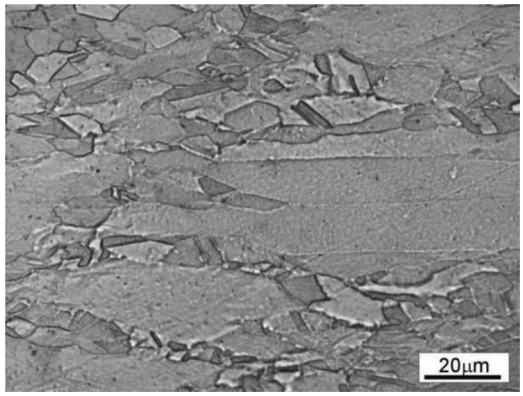

Fig. 8. Microstructure of Inconel 718 alloy forging showing annealed alloy matrix (area 5 on cross-section A of the forging No. 4)

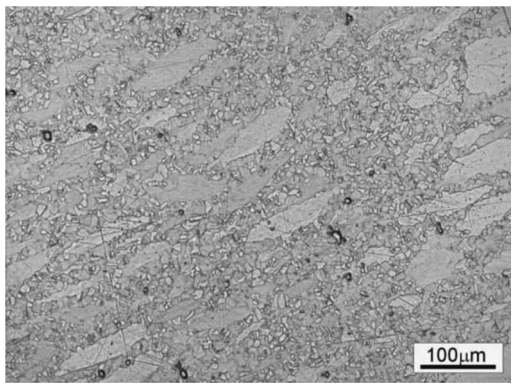

Fig. 9. Undissolved carbides (area 2 on cross-section A of the forging No. 1)

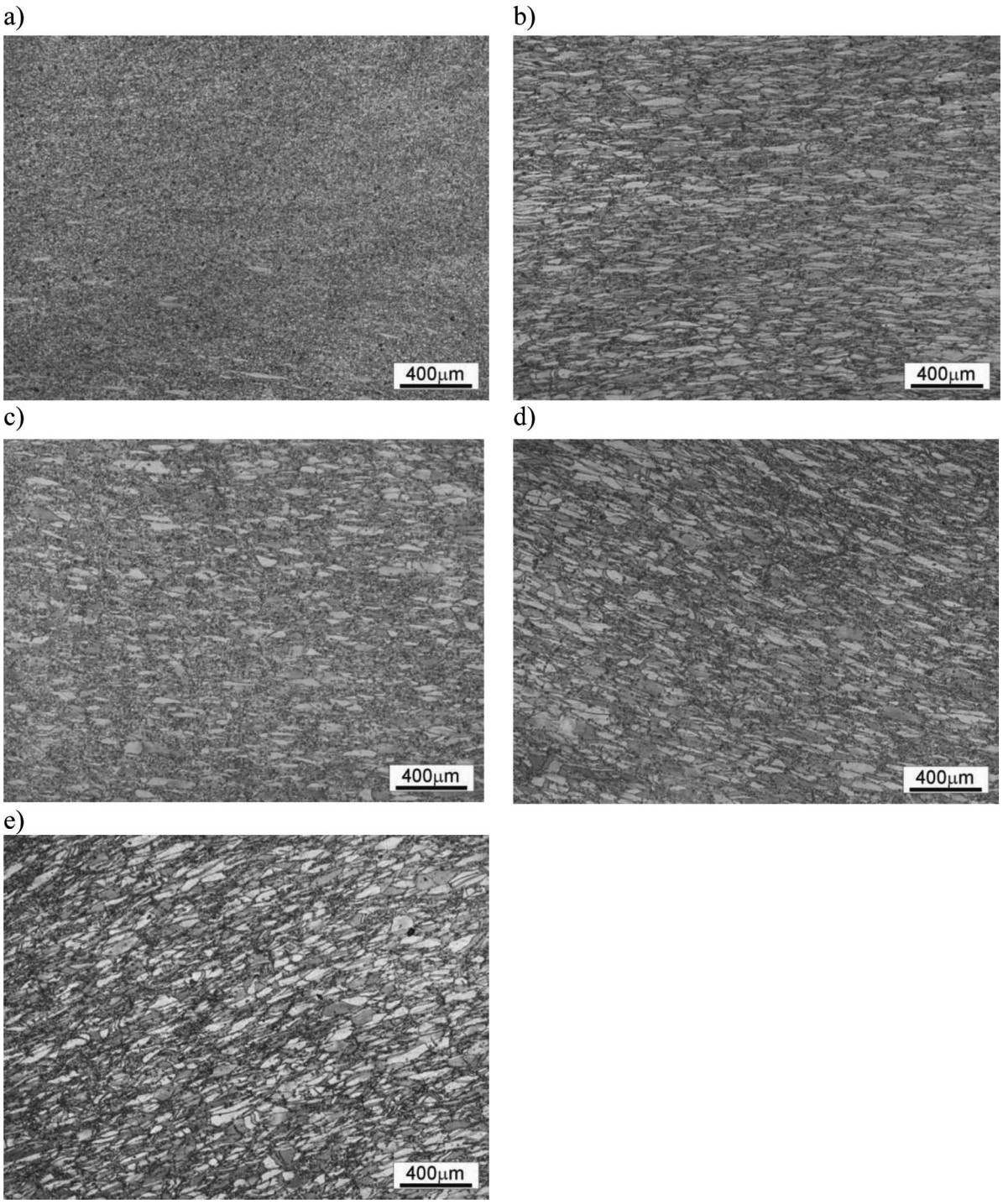

Fig. 10. Changes in the microstructure of the investigated alloy forging indicating an increase of strain in the alloy forging (cross-section A of the forging No. 2): a) area 5, b) area 4, c) area 1, d) area 3, e) area 2

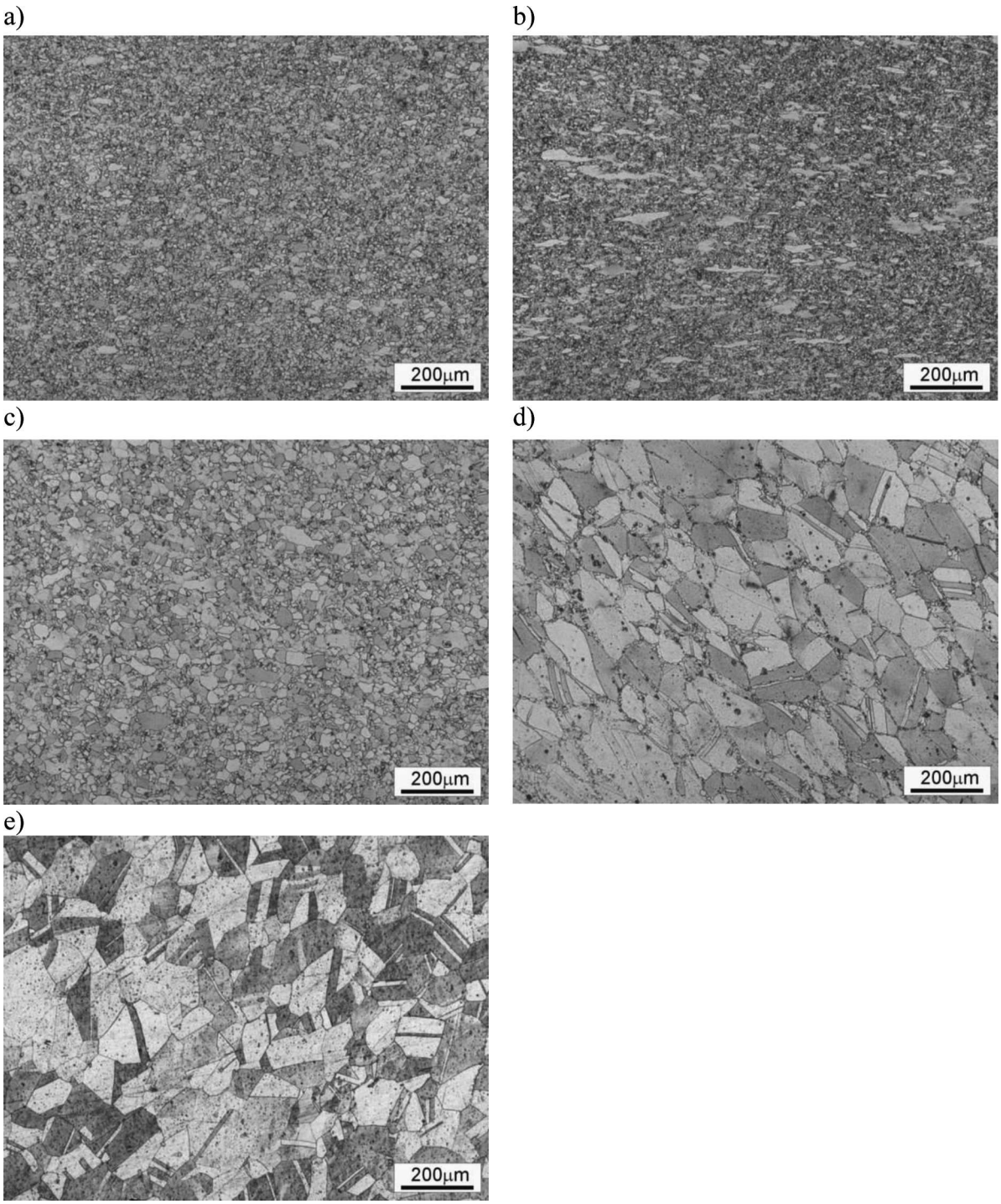

Fig. 11. Changes in the microstructure of the investigated alloy forging indicating an increase of strain in the alloy forging (cross-section B of the forging No. 3): a) area 5, b) area 4, c) area 1, d) area 3, e) area 2

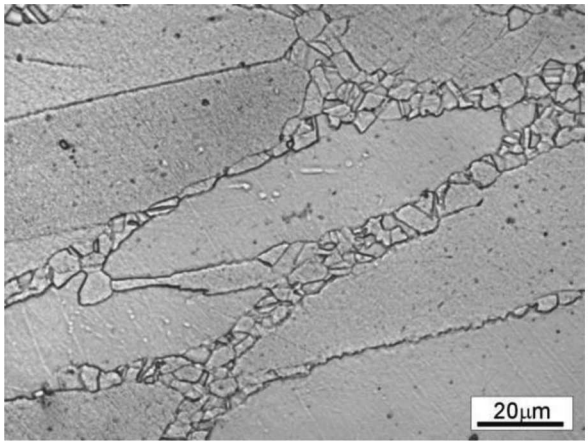

Fig. 12. Nucleation of new, recrystallized grains on the grain boundaries (area 2 on cross-section B of the forging No. 1)

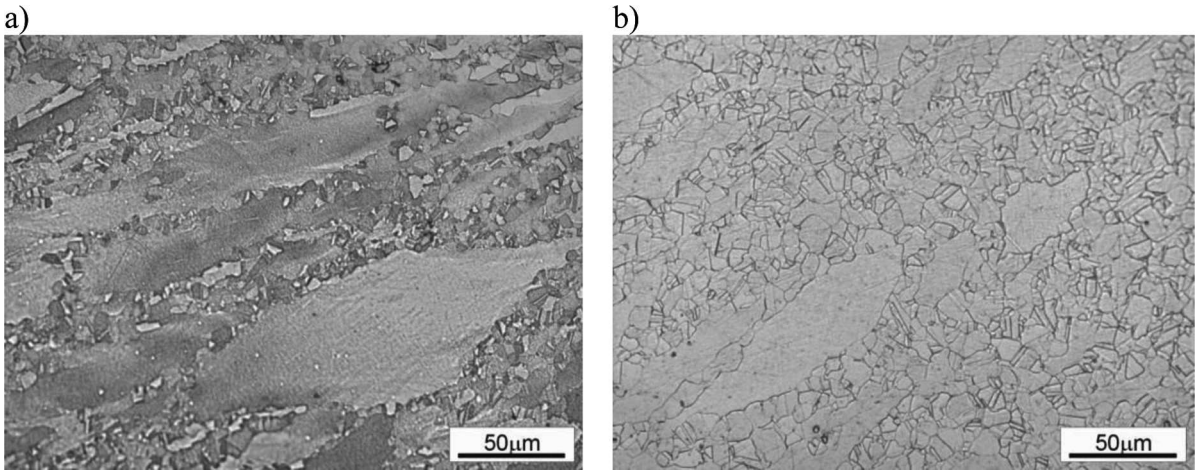

Fig. 13. Differences in the microstructure of the investigated alloy showing the influence of forging temperature on the extend of recrystallization (area 2 on cross-section A): a) forging No. 2 – 1000°C, b) forging No. 1 – 1100°C

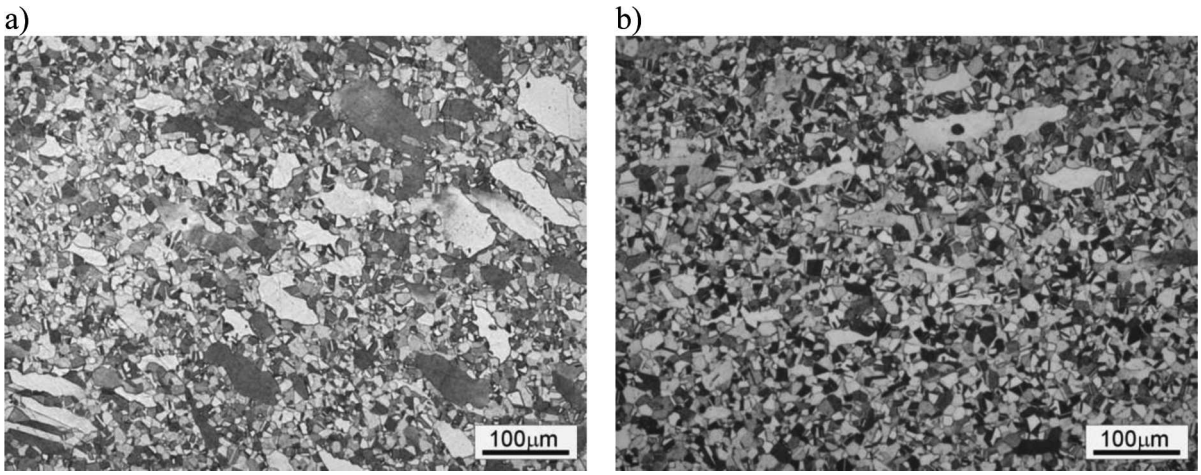

Fig. 14. Differences in the microstructure of the investigated alloy indicating the influence of strain on the extend of recrystallization (cross-section A of the forging No. 1): a) area 3, b) area 5

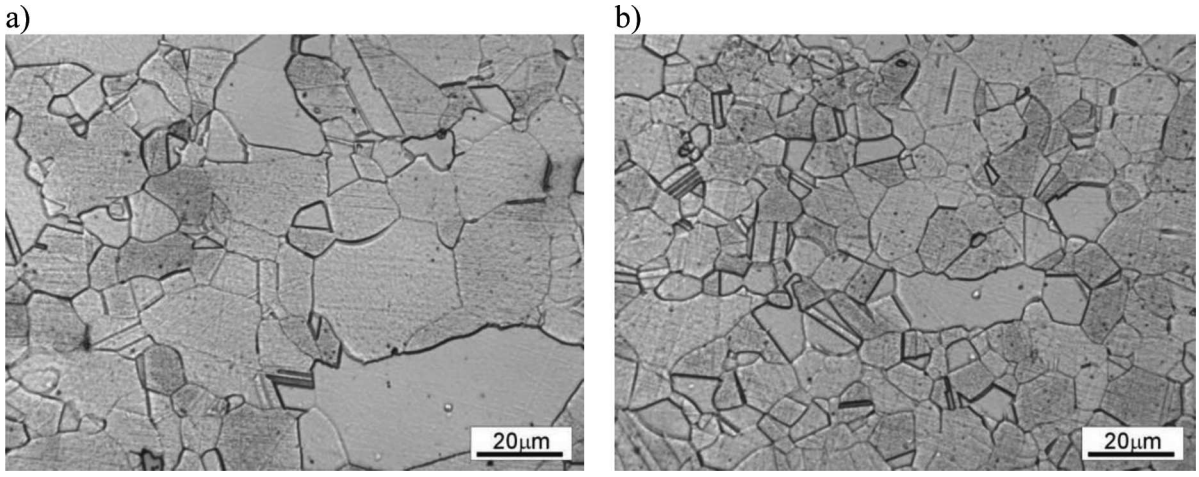

Fig. 15. Differences in the grain size in the investigated alloy indicating different extend of recrystallization resulting from different amount of strain (cross-section B of the forging No. 3): a) area 1, b) area 5

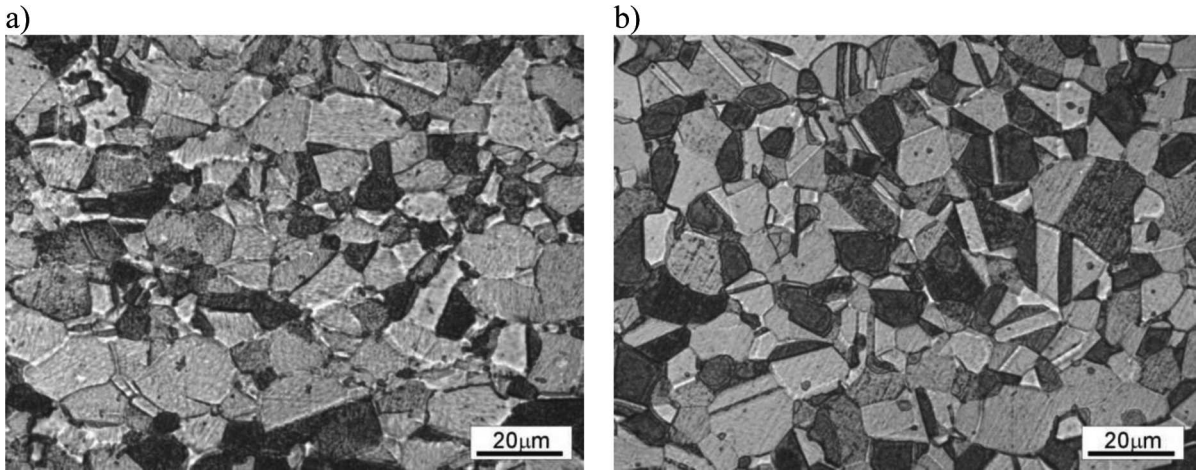

Fig. 16. Differences in the grain size in the investigated alloy indicating different extend of recrystallization resulting from different temperature of forging process (area 5 on cross-section A): a) forging No. 2 – 1000°C, b) forging No. 1 - 1100°C

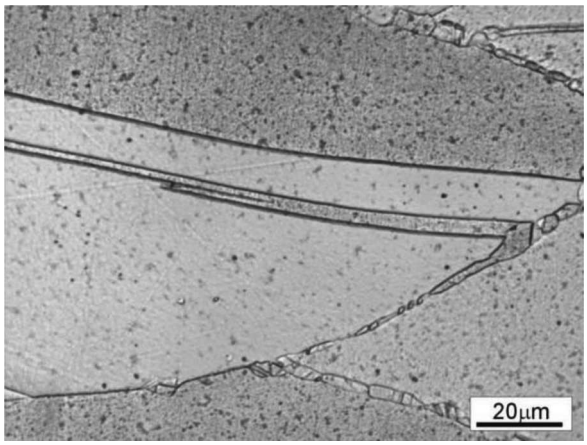

Fig. 17. Microstructure indicating lower susceptibility of twin boundaries to be nucleation sites as compared to grain boundaries (area 1 on cross-section A of the forging No. 4)

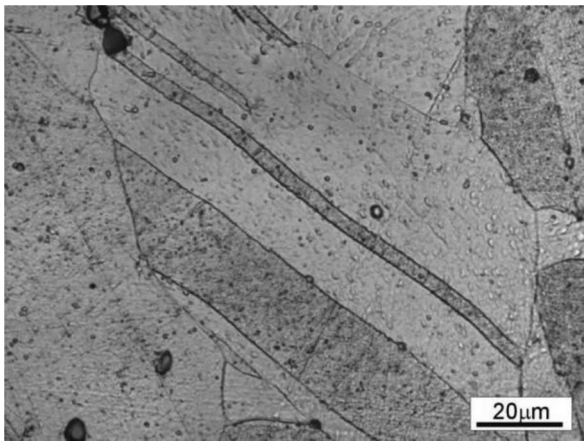

Fig. 18. Microstructure of unrecrystallized area of Inconel 718 alloy (area 3 on cross-section B of the forging No. 4)

The analysis of the microstructure of the forged products showed, that only forgings processed at 1100°C from 30 mm high billet had the most uniform microstructure (forging No. 3).

Hardness of the investigated forgings measured in the areas of metallographic investigations is shown in Figure 19. The smallest spread of average value of hardness on the cross-section of the forged product was obtained in the case of the forging processed at the temperature of 1100°C (forging No. 3). The lowest hardness was measured in the center of the forgings. An increase of the hardness is connected with an increase of strain (highest values were measured at the areas No. 4). Lower temperature of forging caused an increase of hardness of the forged product (300 HV). The hardness of 200 HV was measured only in the forgings processed at higher temperature. Moreover, the hardness distribution were strongly influenced by the extend of recrystallization and subsequent grain growth. Generally, in recrystallized areas of the forgings hardness decreased with the grain growth.

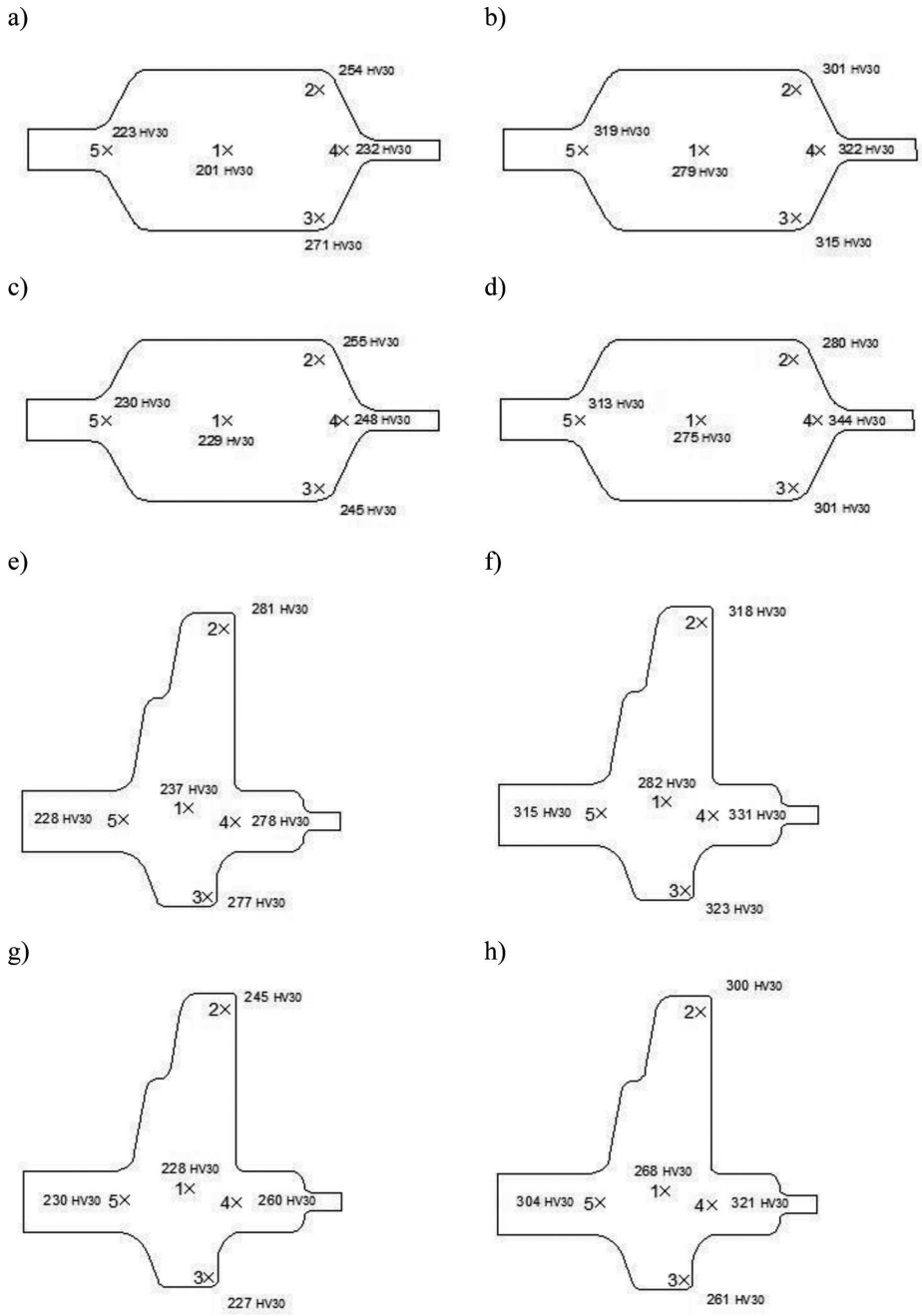

Fig. 19. Hardness of the investigated forgings measured in the areas of metallographic investigations: a) cross-section A – forging No. 1, b) cross-section A – forging No. 2, c) cross-section A – forging No. 3, d) cross-section A – forging No. 4, e) cross-section B – forging No. 1, f) cross-section B – forging No. 2, g) cross-section B – forging No. 3, h) cross-section B – forging No. 4

6. Conclusions

The following conclusions can be drawn from the pre-sent study:

1. The metallographic investigations showed the solutionized microstructure of forged Inconel 718 alloy, with small amount of undissolved carbides, what proved that the parameters of thermomechanical processing of this alloy were properly chosen.
2. Generally, forging process caused recrystallization of the investigated alloy. Some unrecrystallized areas were revealed only in the case of the material forged at 1000°C and in the areas of smallest forging ratio.
3. New, recrystallized grains were formed at prior grain boundaries of the investigated alloy.
4. An increase of the temperature of the billet resulted in more recrystallized microstructure in the forged product.
5. The higher temperature of forging resulted in grain growth in the recrystallized areas of the investigated forgings.
6. Forging of 30 mm high billet at 1100°C resulted in the product of the most uniform microstructure and hardnes distribution of all investigated processing cases.
7. Decrease in strain leads to the grain growth in recrystallized parts of the investigated forgings.

Acknowledgements

Financial support of Structural Funds in the Operational Programme – Innovative Economy (IE OP) financed from the European Regional Development Fund – Project WND-POIG.01.03.01-12-004/09 is gratefully acknowledged.

The authors of this research would like to thank Andrzej Gradzik, Tadeusz Skowronek, Joanna Kowalska, Małgorzata Witkowska, Krzysztof Chruściel, Stanisław Malik, Andrzej Adamczyk for help in the performed investigations.

Received: 10 November 2011.

REFERENCES

[1] M.J. Donachie, S.J. Donachie, Superalloys – A Technical Guide, Second Edition, ASM International 2002.

[2] ASTM B637 – 06, Standard specification for precipitation hardening nickel alloy bars, forgings, and forging stock for high temperature service.

[3] S. Olovjö, A. Wretland, G. Sjöberg, The effect of grain size and hardness of wrought Alloy 718 on the wear of cemented carbide tools, Wear 268, 1045-1052 (2010).

[4] B. Mikułowski, Stopy żaroodporne i żarowytrzymałe – nadstopy, Wydawnictwa AGH, Kraków 1997.

[5] J.R. Davies (red.), Heat-Resistant materials (ASM Specialty Handbook), ASM International 1997.

[6] M. Lachowicz, W. Dudziński, Non equilibrium decomposition of MC carbides in superalloy Inconel 713C melted with welding techniques. Archives of Metallurgy and Materials **55**, 305-315 (2010).

[7] P. Bala, Microstructural characterization of the new tool ni-based alloy with high carbon and chromium content, Archives of Metallurgy and Materials **55**, 1053-1059 (2010).

[8] H.K.D.H. Bhadeshia, Nickel Based Superal-loy. www.msm.cam.ac.uk/phase-trans/2003/superalloys/superalioys.html.

[9] M. Zielinska, J. Sieniawski, M. Yavorska, M. Motyka, Influence of chemical composition of nickel based superalloy on the formation of aluminide coatings. Archives of Metallurgy and Materials **56**, 193-197 (2011).

[10] M. Yavorska, J. Sieniawski, M. Zielinska, Functional properties of aluminide layer deposited on Inconel 713 LC Ni-based superalloy in the CVD process. Archives of Metallurgy and Materials **56**, 187-192 (2011).

[11] M. Wrobel, T. Moskalewicz, J. Krawczyk, M. Blicharski, S. Dymek, Development of microstructure and texture during recrystallization of a Cu-Al single crystal with (100)[011] orientation. Materials Chemistry and Phisics **81**, 524-527 (2002).